https://doi.org/10.1016/j.solmat.2018.03.017

Photovoltaic high-performance broadband photodetector based on MoS_2/Si nanowire array heterojunction

Di Wu[a], Zhenhua Lou[a], Yuange Wang[a], Zhiqiang Yao[b], Tingting Xu[a], Zhifeng Shi[a], Junmin Xu[a], Yongtao Tian[a], Xinjian Li[a,*], and Yuen Hong Tsang[c,*]

[a]Department of Physics and Engineering, and Key Laboratory of Material Physics, Zhengzhou University, Zhengzhou, Henan, 450052, P.R. China

[b]School of Materials Science and Engineering, Zhengzhou University, Zhengzhou, 450052, P. R. China

[c]Department of Applied Physics and Materials Research Center, The Hong Kong Polytechnic University, Hung Hom, Kowloon, Hong Kong, China.

*Author to whom any correspondence should be addressed.

Email: lixj@zzu.edu.cn and yuen.tsang@polyu.edu.hk

Abstract

Photovoltaic MoS_2/Si nanowire array (SiNWA) heterojunction photodetectors (PDs) are constructed and investigated, which exhibit excellent photoresponse properties to light illumination at wavelengths from the deep ultraviolet to the near-infrared. Further photoresponse analysis reveals that a high responsivity of 53.5 A/W and a specific detectivity of 2.8×10^{13} Jones, as well as fast response speeds of 2.9/7.3 μs at 50 kHz are achieved in a MoS_2/SiNWA heterojunction device. The high performances could be attributed to the high-quality heterojunction between MoS_2 and the SiNWA. Such high performances of MoS_2/SiNWA PDs are much better than those of previously reported MoS_2-based PDs, suggesting that MoS_2/SiNWA heterojunction devices have great potential in optoelectronic applications.

Keywords: molybdenum disulfide, heterojunction, Si nanowire arrays, photodetectors, self-powered

1. Introduction

The discovery of graphene has inspired great interest in exploring the promising potential of two-dimensional (2D) layered semiconductor nanostructures for their enormous applications in electronic and optoelectronic devices based on their specific geometries and unique physical properties [1-3]. With atomically thin, stacked with van der Waals force and free of surface chemical dangling bonds, 2D layered semiconductor nanostructures provide an open platform for exploring novel physical phenomena and mechanisms [4, 5]. However, the widespread applications of the pristine graphene in electronics and optoelectronics were limited by its zero band-gap. Transition metal dichalcogenides (TMDs), especially the those with atomic thickness, have been emerged as a new class of nanomaterials for fundamental studies and promising applications due to their distinct properties [6, 7]. Molybdenum disulfide (MoS_2) is one of the most widely studied layered material due to its inherent and layer-dependent band-gaps [8-11]. Crystals of MoS_2 are composed of vertically stacked, weakly interacting layers through van der Waals interactions. When the layers of MoS_2 decreased to monolayer, it will transform to a direct-gap with 1.9 eV from the indirect-gap with 1.2 eV. This unique property grants the great advantages for high-performance devices with high on/off ratio and low power consumption [12-14]. Besides, few-layer MoS_2 can response light signals from ultraviolet (UV) to near infrared (NIR) because of the narrower band-gap, which is beneficial to design a variety of photodetectors (PDs) [15]. All these features revealled that MoS_2 has important potential applications in electronic and optoelectronic devices.

Compared with traditional bulk materials, 2D materials based PDs have several natural advantages, such as wide detection range, free of dangling bonds at the surfaces and strongly interact with incident light [16]. In spite of these advantages, 2D materials based PDs have their drawbacks, such as low absorptivity of incident light, large dark current and small light on/off ratio, and low detectivity. To overcome these drawbacks, diverse device structures and various enhancing methods have been developed. Constructing heterojunction is a promising way to enhanced the device performancs, which can improve the separation efficiency of photoexcited electron-hole pairs [17]. Hence, an increasing interest has been attracted by heterojunction devices of 2D materials [18, 19]. From previous reports, the photoconductor based PDs usually have high responsivities, with slow response speeds, whereas, the junction-based PDs always hold the advantage in fast response speeds [17]. For example, Andras Kis et al. reported a single-layer MoS_2 photoconductor with a high responsivity of 880 A/W, but slow response speeds of 4/9 s (rise/fall time) [20]. Jie et al. reporteded a MoS_2/Si heterojunction PD with fast response speeds of 3/40 μs and a low responsivity of 0.3 A/W [21]. And the similar results were also reported by us and Jiang et al [22, 23]. These heterojunction devices are mainly based on planar Si with poor light harvesting capability, which may lead to the low responsivity. Achieving a high responsivity and a fast response speed simultaneously in a single MoS_2-based PD is an urgently desired for practical optoelectronic applications in the future.

Silicon (Si), one of the most important optoelectronic materials in the

semiconductor industry, is widely used in commercial PDs, PV devices and semiconductor chips due to their high performance as well as the mature large-scale production and integration technologies [24-26]. Si nanostructures, and in particular, Si nanowire arrays (SiNWA) have received increasing attention in recent years due to their unique properties in terms of enhanced light absorption and excellent electron transport characteritic. In addition, enhanced device performances have been demonstrated in PV devices and PDs by using SiNWAs as light harvesting candidates [27-30]. Inspired by these progresses, it is anticipated that combing MoS_2 with SiNWAs may lead to heterojunction PDs with both high responsivities and fast response speeds.

Herein, the photovoltaic MoS_2/SiNWA heterojunction PD was constructed, and its optoelectronic properties were systematically investigated. This PD has exhibited excellent rectifying characteristics and photoresponse properties with pronounced photovoltaic effect. Therefore, it can serve as a self-powered PD, which can operate at voltage bias of 0 V. The photoresponse properties of the MoS_2/SiNWA heterojunction PD were studied, displaying excellent repeatability and stability with high current on/off ratio, high responsivity, specific detectivity, as well as fast response speeds. The method presented in this work is an efficient way to improve the performances of 2D materials based PDs.

2. Experimental Details

2.1 Synthesis and characterization of layered MoS_2 thin films

The few-layer MoS_2 thin films used in this work were fabrictated *via* a thermal

decomposition method, which has been described in our previous work [23, 31]. The crystal structure of the as-fabricated samples were analyzed by an X-ray diffraction (XRD, X' Pert Pro, Panalytical, Netherlands), glancing incidence angle XRD (GIAXRD, SmartLab, Rigaku, Japan) and high-resolution transmission electron microscopy (HRTEM, JEM-2010, JEOL, Japan). X-ray photoelectron spectroscopy (XPS, ESCALAB 250, Thermo Fisher Scientific, USA) was performed to examine the component. Raman spectrum was obtained with a Raman spectroscopy (LabRAM HR Evolution, Horiba, Japan). The thickness was detected by an atomic force microscope (AFM, Dimension Icon, Bruker, USA). Absorption spectra of SiNWAs, and bulk Si were acquired with a UV-VIS-NIR spectrophotometer (UH4150, Hitachi, Japan).

2.2 Construction of the MoS_2/SiNWA heterojunction devices

The vertical ordered SiNWAs were fabricated by etching *n*-type Si wafer with an Ag-assisted chemical etching method [32]. Then, the MoS_2 film was transferred onto the top of SiNWA with a polymethyl methacrylate (PMMA)-assisted process, as demonstrated in Fig. 2c. An electrode of 50 nm Au on the MoS_2 film was defined by a thermal evaporation with a shadow mask. Meanwhile, another electrode of Cu sheet was connected to the cross section of Si substrate *via* high-purity silver conducting paint. A schematic of a MoS_2/SiNWA heterojunction PD was shown in Fig. 3a.

2.3 Device performance characterization

The device performances of PD were investigated with a semiconductor characterization system (Keithley 4200-SCS, Tektronix, USA), combining with a

spectrometer (Omni-λ300, Zolix, China), an oscilloscope (DPO2012B, Tektronix, USA), and a waveform generator (SDG1032X, Siglent, China).

3. Results and Discussions

Fig. 1a shows the XRD and GIAXRD patterns of the as-prepared MoS_2 films on quartz substrates. A strong (002) peak was shown at 2θ =14.3°. In addition, a (105) peak at 2θ = 50.6° and a (106) peak at 2θ = 56.0° were also observed in GIAXRD patterns. From the HRTEM image as shown in Fig. 1b, the MoS_2 has a hexagonal lattice structure with the lattice spacing of 0.27 nm assigned to the (100) and (010) planes. From Raman spectroscopy as shown in Fig. 1c, the layer number of MoS_2 can be identified by the energy difference between the E_{2g} and A_{1g} Raman modes (Δ) [33]. A Δ of 24.0 cm^{-1} indicates that the MoS_2 film is few-layer, which was further confirmed by AFM (~3.1 nm), as shown in Fig. 1d. According to XPS analysis (Fig. 1e and 1f), Mo binding energies of 229.3 and 232.5 eV corresponding to Mo 3d5/2 and Mo 3d3/2, respectively, and S binding energies of 162.2 and 163.3 eV corresponding to 2p3/2 and S 2p1/2 orbitals are observed.

To construct MoS_2/SiNWA heterojunction devices, the SiNWAs were prepared as shown in Fig. 2a. SEM images show that the length of Si nanowires was about 3 μm. Fig. 2b depicts the absorption spectra of the SiNWA and Si wafer. From the curves, the light absorption of the SiNWAs is much enhanced compared to the Si wafer, at the entire UV-VIR-NIR wavelength region, which is beneficial to improve the responsivity of PDs. After obtaining the high-quality few-layer MoS_2 films and SiNWAs, the MoS_2/SiNWA heterojunction devices were fabricated as shown in Fig.

2c.

A schematic of the MoS_2/SiNWA heterojunction device was shown in Fig. 3a. Fig. 3b depicts the current-voltage (*I*-*V*) curves of the MoS_2/SiNWA and MoS_2/bulk Si heterojunction devices in the dark and under light illuminations of 650 nm with an intensity of 38.6 mW cm^{-2}. From which, the excellent rectification characteristic of the MoS_2/SiNWA heterojunciton with a rectification ratio up to 10^2 within ±5 V can be obtained in the dark. For an ideal diode, the I-V characteristic can be described by the following equation:

$$I = I_0(e^{qV_{DS}/nk_BT} - 1) \quad (1)$$

Therefore, the ideality factor n can be expressed as:

$$n = \frac{q}{K_B T}\frac{dV}{d\ln I} \quad (2)$$

where I_0, K_B and T represent the reverse bias leakage current, the Boltzmann constant and the temperature in Kelvin, respectively. By fitting the rectification curve, a small ideality factor n of 1.05 can be obtained in the low-bias zone, which is consistent with the theoretical value (n = 1) [34]. Under light irradiation, the current became strong in both forward and reverse directions, leading to a high current on/off ratio (I_{on}/I_{off}) over 10^3 at -5 V. It is worth noting that the dark current of the MoS_2/SiNWA device is much lower than the value of the MoS_2/bulk Si device, whereas the photocurrent of the MoS_2/SiNWA device is much larger than that of the MoS_2/bulk Si device. It is believed that the contact area of MoS_2 and Si, and the higher absorptivity of incident light of SiNWA are responsible for these differences.

Moreover, pronounced photovoltaic behaviors were observed under light

illumination of 650 nm, and an open-circuit photovoltage (V_{OC}) of 0.29 V and short circuit current (I_{SC}) of 18.6 μA were obtained at a light intensity of 38.6 mW cm^{-2} (Inset of Fig. 3b). Therefore, this MoS_2/SiNWA heterojunction device can serve as a self-powered PD. The photoresponse of MoS_2/SiNWA PD under different bias voltages were investigated, as shown in Fig. 3c. The stable and repeatable photoresponse with different I_{on}/I_{off} ratios can be observed when the light (650 nm, 38.6 mW cm^{-2}) was turned on and off. The I_{on}/I_{off} ratios can be deduced to 1.1×10^5, 3.6×10^2, 7.5×10^2 and 3.0×10^3 under bias voltages of 0 V, -1 V, -2 V and -5 V, respectively, which are much larger than 3.15×10^2 of MoS_2/bulk Si heterojunction devices, and values reported previously [21, 23]. Fig. 3d shows the response spectrum of the MoS_2/SiNWA PD, from which, an obvious photoresponse over a wide wavelength range from UV to NIR (300-1200 nm) can be observed. Moreover, the striking response properties to deep UV of 250 nm and NIR of 1200 nm at voltage bias of 0 V were shown in Fig. 3e and f, indicating that such MoS_2/SiNWA heterojunction PD has great potential application in broadband photodetection.

Light intensity is a key factor that determines the photocurrent in PDs. The light intensity-dependent photoresponse of the MoS_2/SiNWA PD were further studied as shown in Fig. 4a. It depicts that the I-V curves of the MoS_2/SiNWA PD under varied light intensities from dark to 38.6 mW cm^{-2}. The I_{SC} is highly dependent on the light intensity and increase with increasing light intensity. The I_{SC} *versus* the light intensity was plotted in Fig. 4b, which can be described as:

$$I=AP^{\alpha} \quad (3)$$

where A is a constant. The exponent α, which determines the response of the photocurrent to light intensity, can be determined to be 0.8. This fractional power dependence is believed to be related to the carrier trap states between the Fermi level and the conduction band edge [35]. The photoresponses of MoS_2/SiNWA PD at zero bias under different light intensities were also investigated, as shown in Fig. 4c. From the curves, stable and repeatable photoresponses with high I_{on}/I_{off} ratios of 3.2×10^2, 2.9×10^3, 2.8×10^4 and 1.1×10^5 could be obtained under light intensities of 0.031, 0.46, 4.5 and 32 mW cm^{-2}, respectively. As two important parameters of PD, responsivity (R) and specific detectivity (D*) can be calculated according to the following relations:

$$R = \frac{I_P - I_d}{P_{opt} \cdot S} \tag{4}$$

$$D^* = \frac{\sqrt{A}R}{\sqrt{2eI_d}} \tag{5}$$

where I_p, I_d, P_{opt}, S and A are the photocurrent, dark current, the incident light intensity, the area of light illumination and device area, respectively. Hence, the light intensity-dependent responsivity and specific detectivity are shown in Fig. 4d. Both R and D* increased with the decreasing light intensity and can be estimated to be 53.5 A/W and 2.8×10^{13} Jones (1 Jones =1 cm $Hz^{1/2}$ W^{-1}) under a light intensity of 6.3 μW cm^{-2}, which are much larger than the values obtained for the MoS_2/bulk Si device.[23] Another figure of merit for PD is the linear dynamic range (LDR), which is defined by the following equation:[16]

$$LDR = 20log\frac{I_P^*}{I_d} \tag{6}$$

where I_P* represents the photocurrent measured at a light intensity of 1 mW cm^{-2}. A LDR of 72.8 dB at zero bias can be obtained, which is better than 42 dB of WS_2/n-Si, and 66 dB of the commercialized InGaAs photodiodes [36-38].

The response speed is another key parameter for PDs, representing their ability to monitor quick varying optical signals. In this work, the photoresponse properties of the MoS_2/SiNWA PD were further evaluated by modulating the frequency of the incident light with a waveform generator. And the photocurrent was monitored by an oscilloscope with time, as shown in Fig. 5. Fig. 5a-c show the repetitive switching of the PD between low and high conduction states when the laser diode was turned on and off regularly at frequencies of 500 Hz, 3000 Hz and 10 kHz, respectively. From the figure, the MoS_2/SiNW PD could operate with excellent stability and repeatability over a wide frequency range up to 150 kHz under a light intensity of 38.6 mW cm^{-2}. Moreover, the relative balance $[(I_{max}-I_{min})/I_{max}]$ of the photocurrent can remain at 77% under a high frequency of 10 kHz, implying that this MoS_2/SiNW PD is capable of monitoring ultrafast optical signals. The 3 dB bandwidth (f_{3dB}) of 13 kHz can be obtained from Fig. 5d, which is much large than the values of some reported PDs [39, 40]. In the time domain, the response speed of PDs is usually defined by the rise time (τ_r) and the fall time (τ_f). From further analysis, a small τ_r of 22.8 μs and τ_f of 61.5 μs were obtained at 4 kHz and 2.9/7.3 μs at 50 kHz, which are superior to or close to previous results [22, 41].

Moreover, light intensity has been found to greatly influence the response speed [42]. Hence, the response speed of a MoS_2/SiNWA PD was investigated under varied

light intensities at a frequency of 4 kHz, as shown in Fig. 6. Rise times of 54.2, 27.7, 23.5 and 22.8 μs, and fall times of 69.9, 68.6, 67.4 and 61.5 μs were observed under light intensities of 2.5, 16.8, 24.5 and 38.6 mW cm^{-2}, respectively. It is worth noting that the rise/fall time decreased with the increase in the incident light intensity. The reduction of the time constants with increasing light intensity is in good agreement with Rose's model [43]. To investigate the repeatability of this device, device performance of five MoS_2/SiNWA PDs, which were fabricated by the same process and technology, were summarized in Table 1, demonstrating that these devices showed similar device performances, proving that our devices have good repeatability. Table 2 summarized the device performances of the MoS_2/SiNWA PD and some reported PDs. It is important to note that when Si substrate was replaced by SiNWAs, the response speed maintained almost the same value, but the responsivity and specific detectivity were much enhanced.

The internal resistance (R) and capacitance (C) of MoS_2/Si heterojunction device were investigated by electrical impedance spectroscopy (EIS). The simplified equivalent circuit including the internal R and C are proposed to evaluate the interface quality, as illustrated in Fig. 8a. The Nyquist plots of the MoS_2/Si heterojunction was investigated in the dark with an applied voltage of 0.06 V. The resistance R_S, R_{pn} and $R_{Cu/Si}$ are estimated to be 2.4×10^3 Ω, 1.9×10^6 Ω and 1.4×10^4 Ω, respectively. Additionally, the capacitance C_{pn} is obtained to 6×10^{-9} F. The small R_S is beneficial to transfer carrier, leading to larger photocurrent. And the high R_{pn} can effectively suppress the charge recombination, which will improve the device performance.

The fast response speed of MoS_2/SiNWA PD is believed to be related to the high-quality heterojunction between the MoS_2 and the SiNWA. The electron affinities of MoS_2 and Si are ~4.3 eV and ~4.05 eV, and their band-gap values are known to be ~1.3 eV (MoS_2) and ~1.12 eV (Si) [12, 22, 44, 45], respectively. Such electronic structures will decide the conduction and valence band offsets between the two semiconductors being ~0.25 and ~0.33 eV, as shown in Fig. 7. When MoS_2 contacts with Si, a typical n-n junction is formed [46]. Due to the ~250 meV for the conduction band edge, MoS_2 is more negative than Si, and electrons would diffuse into MoS_2 from Si, while holes would diffuse into Si from MoS_2. As a result, a built-in electric field would be formed at the MoS_2/Si interface. When the device was exposed to light with engeries larger than the band-gap of the semiconductors, absorption of the incident light would result in the generation of excitons on both the MoS_2 and Si sides. Once the excitons diffuse into the interface of the junction, they are separated in opposite directions by the built-in electric field at the interface. The electrons would inject into MoS_2, while the holes would drift to Si, leading to the fast response speed and giving rise to the photocurrent in the external circuit. The built-in electric field would reduce electron-hole recombination and prevent the transport of electrons from the MoS_2 into Si, leading to a low reverse dark current and thus improving the detectivity. Moreover, the built-in potential at the interface would allow device operate at zero bias voltage, realizing the self-powered property.

4. Conclusions

In summary, large-scale few-layer MoS_2 thin films were synthesized *via* a thermal

decomposition method, and SiNWAs were obtained by Ag-assisted chemical etching method. MoS_2/SiNWA heterojunction devices were fabricated and investigated, which exhibited pronounced photoresponse and photovoltaic properties. Further photoresponse analysis revealled that such MoS_2/SiNWA PDs can work under zero bias with high photosensitivities and fast response speeds. It is most important that a high responsivity of 53.5 A/W, a specific detectivity of 2.8×10^{13} Jones and a fast response speed of 2.9/7.3 μs were achieved in a single device. The approach demonstrated here could be extended to the study of other 2D materials-based heterojunctions for high-performance PDs and may offer new possibilities toward practical optoelectronic applications.

Acknowledgements

This work was supported by the National Natural Science Foundation of China (Nos. 61605174, 11504331), the China Postdoctoral Science Foundation (No. 2015M582194), the Key Projects of Higher Education in Henan Province (No. 17A140012), the Startup Research Fund of Zhengzhou University (1512317002), and Research Grants Council of Hong Kong, China (Project Number: GRF 152109/16E PolyU B-Q52T).

References

[1] C. Tan, X. Cao, X.J. Wu, Q. He, J. Yang, X. Zhang, J. Chen, W. Zhao, S. Han, G.H. Nam, M. Sindoro, H. Zhang, Chem. Rev. 117 (2017) 6225-6331.

[2] M. Xu, T. Liang, M. Shi, H. Chen, Chem. Rev. 113 (2013) 3766-3798.

[3] Z. Zhu, X. Cai, S. Yi, J. Chen, Y. Dai, C. Niu, Z. Guo, M. Xie, F. Liu, J.H. Cho, Y. Jia, Z. Zhang, Phys. Rev. Lett. 119 (2017) 106101.

[4] M. Chhowalla, D. Jena, H. Zhang, Nat. Rev. Mater. 1 (2016) 16052.

[5] Q.H. Wang, K. Kalantar-Zadeh, A. Kis, J.N. Coleman, M.S. Strano, Nat. Nanotechnol. 7 (2012) 699-712.

[6] D. Jariwala, V.K. Sangwan, L.J. Lauhon, T.J. Marks, M.C. Hersam, ACS Nano 8 (2014) 1102-1120.
[7] K. Chen, X. Wan, J. Xu, Adv. Funct. Mater. 27 (2017) 1603884.
[8] K.F. Mak, C. Lee, J. Hone, J. Shan, T.F. Heinz, Phys. Rev. Lett. 105 (2010) 136805.
[9] C. Ahn, J. Lee, H.U. Kim, H. Bark, M. Jeon, G.H. Ryu, Z. Lee, G.Y. Yeom, K. Kim, J. Jung, Y. Kim, C. Lee, T. Kim, Adv. Mater. 27 (2015) 5223-5229.
[10] B. Radisavljevic, A. Radenovic, J. Brivio, V. Giacometti, A. Kis, Nat. Nanotechnol. 6 (2011) 147-150.
[11] Z. Lou, D. Wu, K. Bu, T. Xu, Z. Shi, J. Xu, Y. Tian, X. Li, J. Alloys Compd. 726 (2017) 632-637.
[12] S. Kim, A. Konar, W.-S. Hwang, J.H. Lee, J. Lee, J. Yang, C. Jung, H. Kim, J.-B. Yoo, J.-Y. Choi, Y.W. Jin, S.Y. Lee, D. Jena, W. Choi, K. Kim, Nat. Commun. 3 (2012) 1011.
[13] B. Radisavljevic, M.B. Whitwick, A. Kis, ACS Nano 5 (2011) 9934-9938.
[14] C.-J. Shih, Q.H. Wang, Y. Son, Z. Jin, D. Blankschtein, M.S. Strano, ACS Nano 8 (2014) 5790-5798.
[15] W. Choi, M.Y. Cho, A. Konar, J.H. Lee, G.-B. Cha, S.C. Hong, S. Kim, J. Kim, D. Jena, J. Joo, S. Kim, Adv. Mater. 24 (2012) 5832-5836.
[16] J. Wang, H. Fang, X. Wang, X. Chen, W. Lu, W. Hu, Small 13 (2017) 1700894.
[17] C. Xie, C. Mak, X. Tao, F. Yan, Adv. Funct. Mater. 27 (2017) 1603886.
[18] Y. Liu, N.O. Weiss, X. Duan, H.-C. Cheng, Y. Huang, X. Duan, Nat. Rev. Mater. 1 (2016) 16042.
[19] R. Zhuo, Y. Wang, D. Wu, Z. Lou, Z. Shi, T. Xu, J. Xu, Y. Tian, X. Li, J. Mater. Chem. C 6 (2018) 299-303.
[20] O. Lopez-Sanchez, D. Lembke, M. Kayci, A. Radenovic, A. Kis, Nat. Nanotechnol. 8 (2013) 497-501.
[21] L. Wang, J. Jie, Z. Shao, Q. Zhang, X. Zhang, Y. Wang, Z. Sun, S.T. Lee, Adv. Funct. Mater. 25 (2015) 2910-2919.
[22] Y. Zhang, Y. Yu, L. Mi, H. Wang, Z. Zhu, Q. Wu, Y. Zhang, Y. Jiang, Small 12 (2016) 1062-1071.
[23] Z. Lou, L. Zeng, Y. Wang, D. Wu, T. Xu, Z. Shi, Y. Tian, X. Li, Y.H. Tsang, Opt. Lett. 42 (2017) 3335.
[24] R.A. Soref, Proceedings of the IEEE 81 (1993) 1687-1706.
[25] M. Casalino, G. Coppola, M. Iodice, I. Rendina, L. Sirleto, Sensors (Basel) 10 (2010) 10571-10600.
[26] Z. Shi, D. Wu, T. Xu, Y. Zhang, B. Zhang, Y. Tian, X. Li, G. Du, J. Phys. Chem. C 120 (2016) 4504-4510.
[27] K. Yong Ko, H. Kang, W. Lee, C.-W. Lee, J. Park, H.S. Lee, S. Im, H.-G. Kim, S.-H. Kim, B.-W. Min, H. Kim, Mater. Sci. Semicond. Process. 33 (2015) 154-160.
[28] K.Y. Ko, H. Kang, J. Kim, W. Lee, H.S. Lee, S. Im, J.Y. Kang, J.-M. Myoung, H.-G. Kim, S.-H. Kim, H. Kim, Mater. Sci. Semicond. Process. 27 (2014) 297-302.
[29] C. Xie, B. Nie, L. Zeng, F.-X. Liang, M.-Z. Wang, L. Luo, M. Feng, Y. Yu, C.-Y. Wu, Y. Wu, S.-H. Yu, ACS Nano 8 (2014) 4015-4022.
[30] C. Xie, L.-B. Luo, L.-H. Zeng, L. Zhu, J.-J. Chen, B. Nie, J.-G. Hu, Q. Li, C.-Y. Wu, L. Wang, J.-S. Jie, CrystEngComm 14 (2012) 7222.
[31] D. Wu, Z. Lou, Y. Wang, T. Xu, Z. Shi, J. Xu, Y. Tian, X. Li, Nanotechnology 28 (2017) 435503.
[32] K. Peng, H. Fang, J. Hu, Y. Wu, J. Zhu, Y. Yan, S. Lee, Chemistry 12 (2006) 7942-7947.
[33] K.K. Liu, W. Zhang, Y.H. Lee, Y.C. Lin, M.T. Chang, C.Y. Su, C.S. Chang, H. Li, Y. Shi, H. Zhang, C.S. Lai, L.J. Li, Nano Lett. 12 (2012) 1538-1544.

[34] D. Wu, Y. Jiang, S.Y. Li, F.Z. Li, J.W. Li, X.Z. Lan, Y.G. Zhang, C.Y. Wu, L.B. Luo, J.S. Jie, Nanotechnology 22 (2011) 405201-405206.
[35] S.-C. Kung, W.E. van der Veer, F. Yang, K.C. Donavan, R.M. Penner, Nano Lett. 10 (2010) 1481-1485.
[36] C.O. Kim, S. Kim, D.H. Shin, S.S. Kang, J.M. Kim, C.W. Jang, S.S. Joo, J.S. Lee, J.H. Kim, S.H. Choi, E. Hwang, Nat. Commun. 5 (2014) 3249.
[37] P. Wang, S. Liu, W. Luo, H. Fang, F. Gong, N. Guo, Z.G. Chen, J. Zou, Y. Huang, X. Zhou, J. Wang, X. Chen, W. Lu, F. Xiu, W. Hu, Adv. Mater. 29 (2017) 1604439.
[38] R.K. Chowdhury, R. Maiti, A. Ghorai, A. Midya, S.K. Ray, Nanoscale 8 (2016) 13429-13436.
[39] D. Wu, Y. Jiang, Y.G. Zhang, J.W. Li, Y.Q. Yu, Y.P. Zhang, Z.F. Zhu, L. Wang, C.Y. Wu, L.B. Luo, J.S. Jie, J. Mater. Chem. 22 (2012) 6206-6212.
[40] L. Gao, C. Chen, K. Zeng, C. Ge, D. Yang, H. Song, J. Tang, Light: Science & Applications 5 (2016) e16126.
[41] D.-S. Tsai, K.-K. Liu, D.-H. Lien, M.-L. Tsai, C.-F. Kang, C.-A. Lin, L.-J. Li, J.-H. He, ACS Nano 7 (2013) 3905-3911.
[42] Y. Jiang, W.J. Zhang, J.S. Jie, X.M. Meng, X. Fan, S.T. Lee, Adv. Funct. Mater. 17 (2007) 1795-1800.
[43] A. Rose, Concepts in Photoconductivity and Allied Problems, Interscience Publishers, 1963; p 1239-1243.
[44] B. Evans, Optical Properties of layer compounds. In *Optical and Electrical Properties*, Springer: 1976; pp 1-143.
[45] W. Mönch, Appl. Phys. Lett. 72 (1998) 1899-1901.
[46] J.P. Jiang, C.C. Sun, Heterojunction principles and devices, Publishing house of electronics industry, Beijing, 2010.
[47] C. Chen, Z. Feng, Y. Feng, Y. Yue, C. Qin, D. Zhang, W. Feng, ACS Appl. Mater. Interfaces 8 (2016) 19004-19011.
[48] L. Ye, H. Li, Z. Chen, J. Xu, ACS Photonics 3 (2016) 692-699.
[49] C. Lan, C. Li, S. Wang, T. He, T. Jiao, D. Wei, W. Jing, L. Li, Y. Liu, ACS Appl. Mater. Interfaces 8 (2016) 18375-18382.
[50] X. Li, M. Zhu, M. Du, Z. Lv, L. Zhang, Y. Li, Y. Yang, T. Yang, X. Li, K. Wang, H. Zhu, Y. Fang, Small 12 (2016) 595-601.

Figures

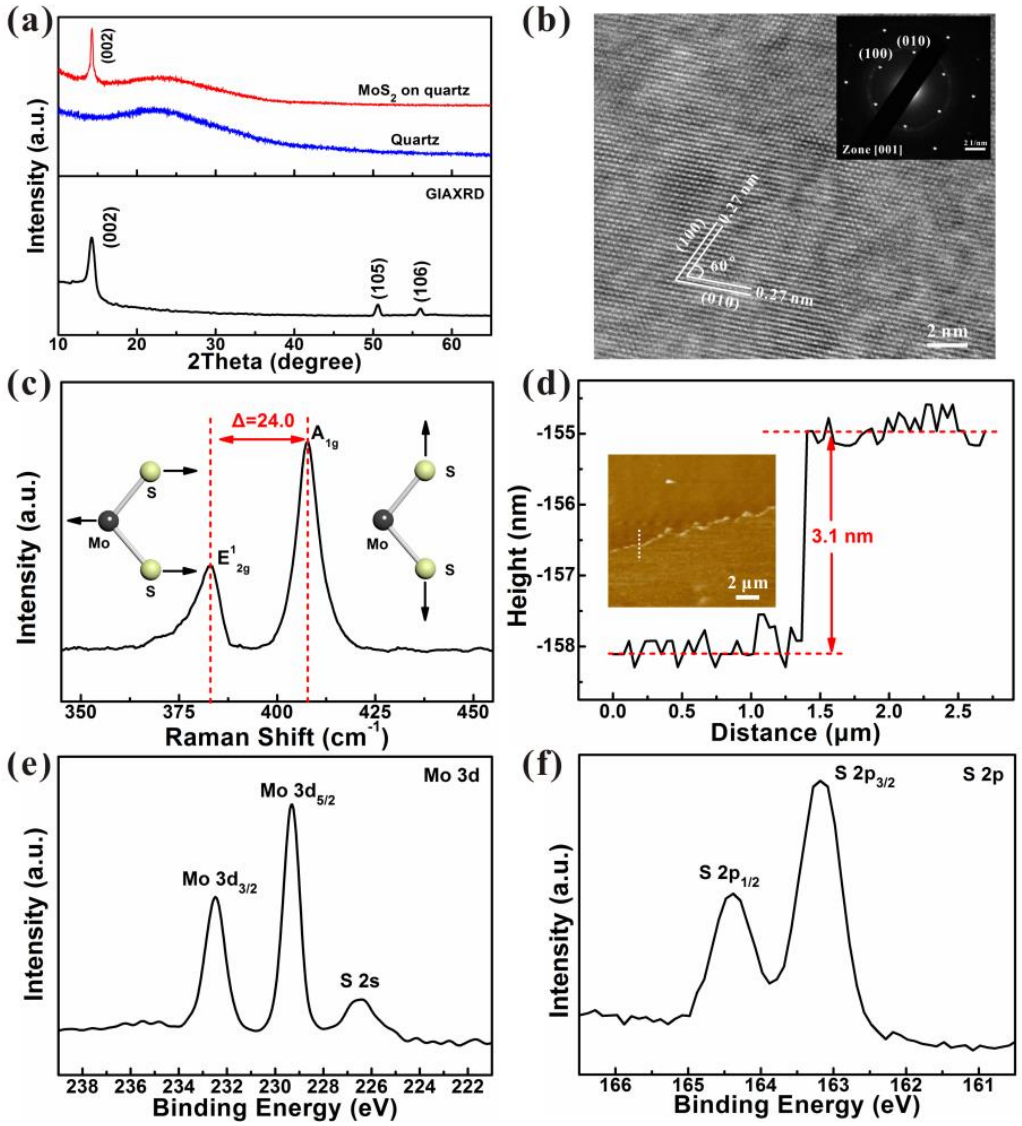

Fig. 1. (a) XRD and GIAXRD patterns of MoS_2 thin film. (b) HRTEM and corresponding SAED pattern of MoS_2 thin film. (c) Raman spectrum, and (d) height profiles of a MoS_2 thin film. The XPS spectra show the binding energies of (e) Mo and (f) S of the MoS_2 thin film.

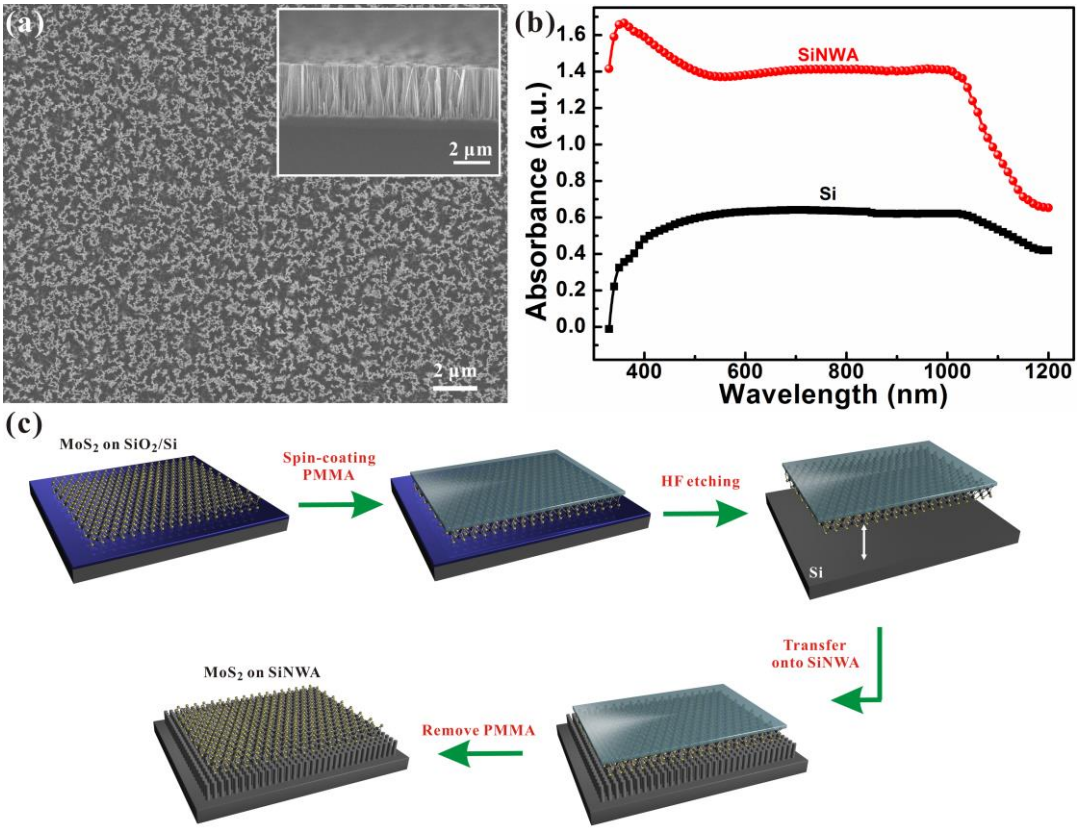

Fig. 2. (a) SEM images of the SiNWA, inset shows the cross-section image. (b) Absorption spectra of a SiNWA and bulk Si substrate. (c) Schematic diagram of a MoS_2/SiNWA heterojunction device fabrication.

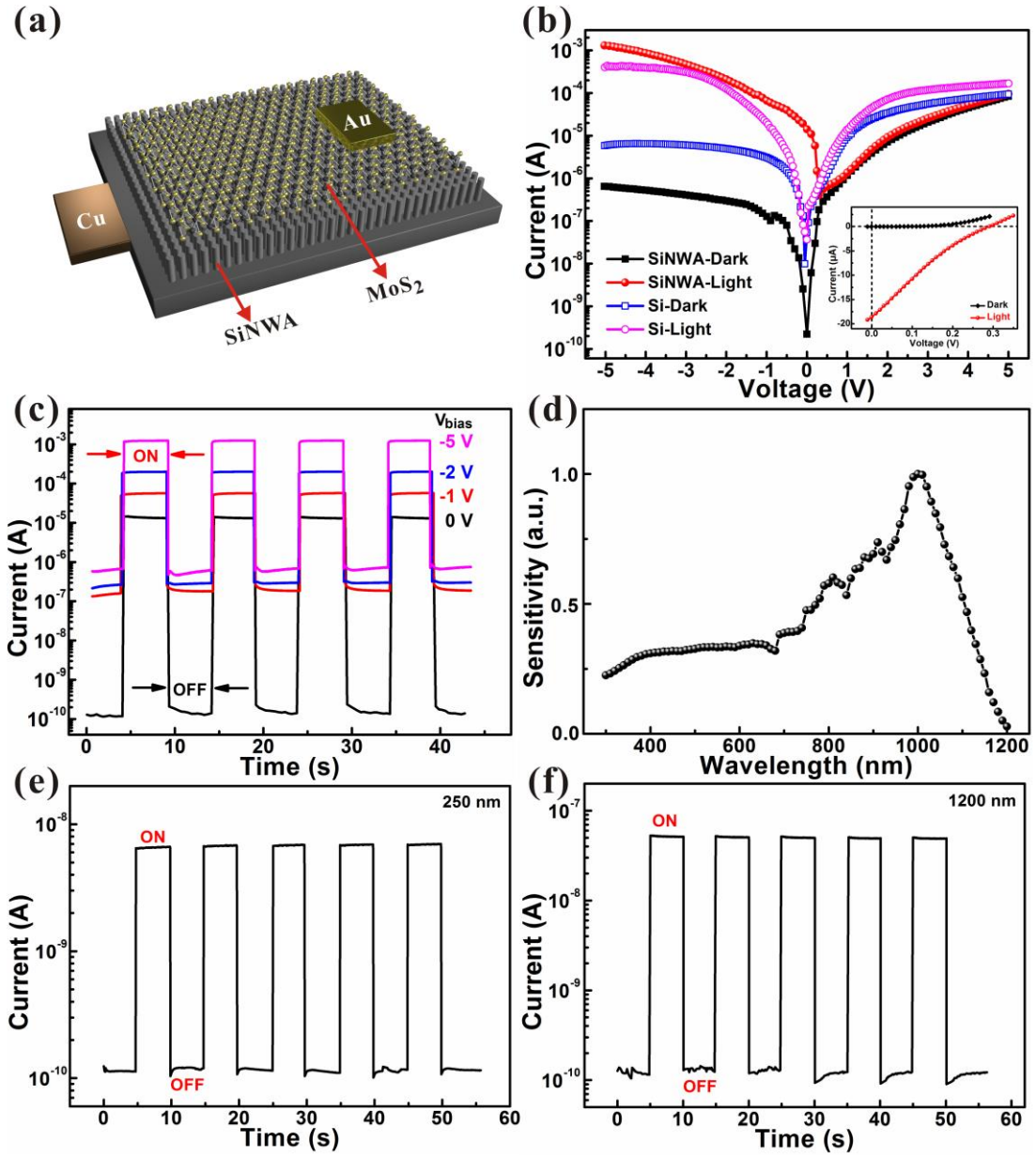

Fig. 3. (a) Schematic illustration of a MoS_2/SiNWA heterojunction device. (b) I-V curves of MoS_2/Si and MoS_2/SiNWA heterojunction devices in the dark and under light illumination (650 nm). Inset shows the photovoltaic effect of the MoS_2/SiNWA heterojunction device. (c) Photoresponse of the MoS_2/SiNWA heterojunction under different bias voltages. (d) The sensitivities of the MoS_2/SiNWA and MoS_2/Si PDs as a function of wavelength. Photoresponse of the MoS_2/SiNWA heterojunction under incident light of (e) 250 nm (1.2 μW/cm^2) and (f) 1200 nm (100 μW/cm^2) at voltage bias of 0 V.

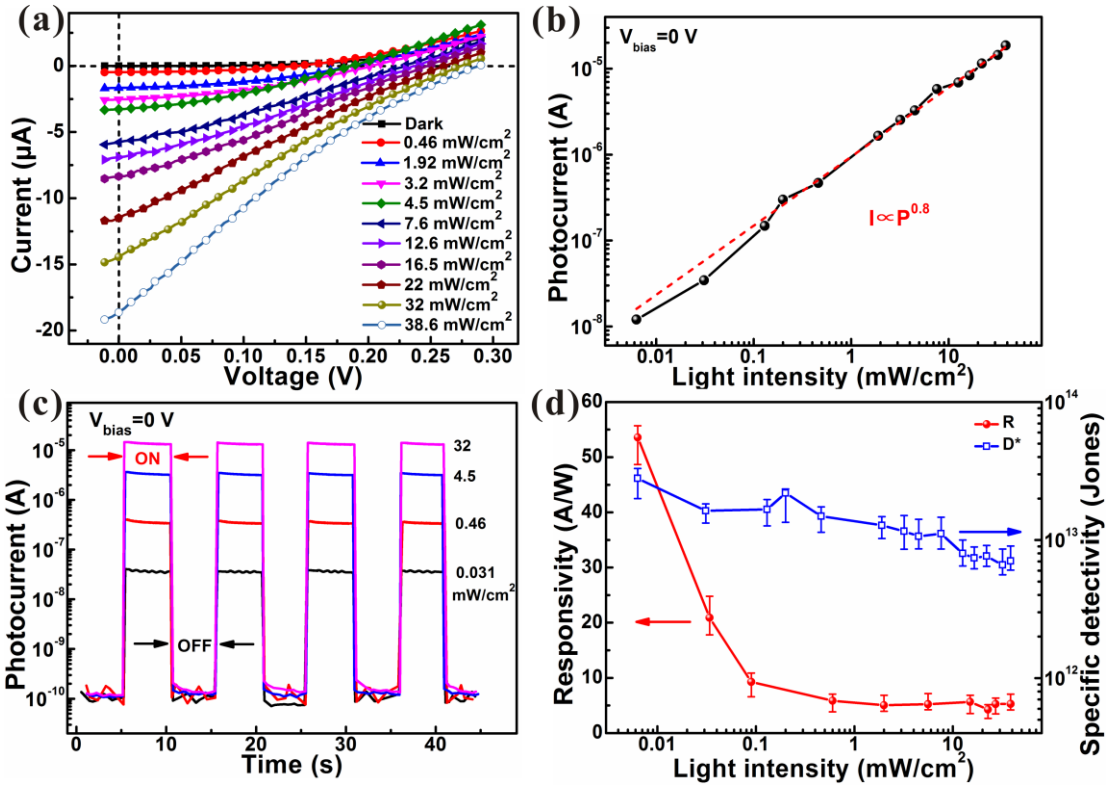

Fig. 4. (a) Photovoltaic properties of the MoS_2/SiNWA heterojunction at varied light intensities (650 nm). (b) Logarithmic plot of the photocurrent *vs* light intensity. The curve is fitted well by the power law. (c) Photoresponse of the MoS_2/SiNWA heterojunction under varied light intensity. (d) Light intensity-dependent responsivity and specific detectivity.

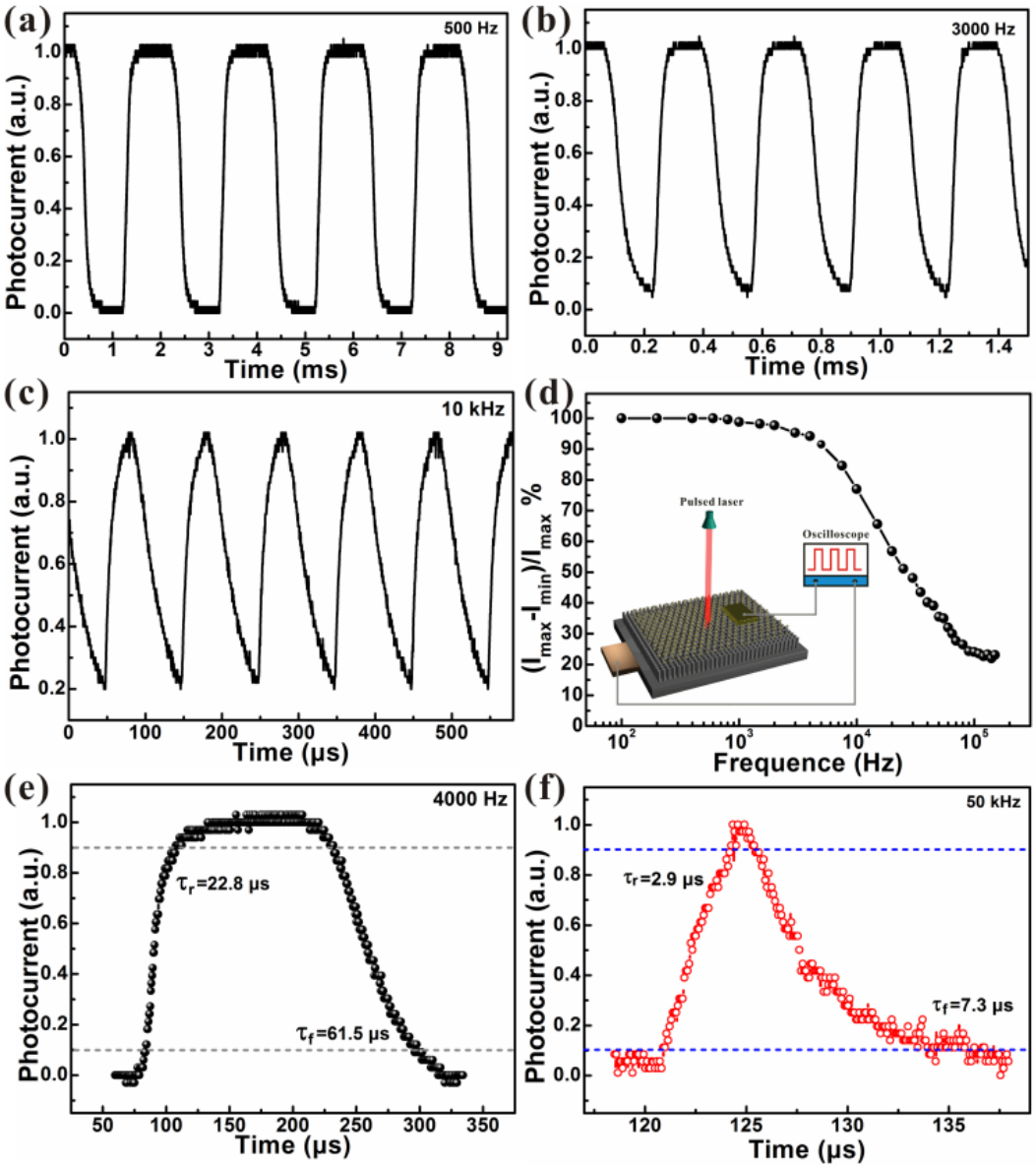

Fig. 5. Photoresponse characteristics of the MoS_2/SiNWA heterojunction to pulsed light irradiation at frequencies of (a) 500 Hz, (b) 3000 Hz and (c) 10 kHz at a voltage of 0 V. (d) The relative balance $[(I_{max}-I_{min})/I_{max}]$ vs switching frequency, inset shows the schematic illustration of the measurement configuration for photoresponse detection. Rising and falling edges for estimating rise time (τ_r) and the fall time (τ_f) at (e) 4 kHz and (f) 50 kHz.

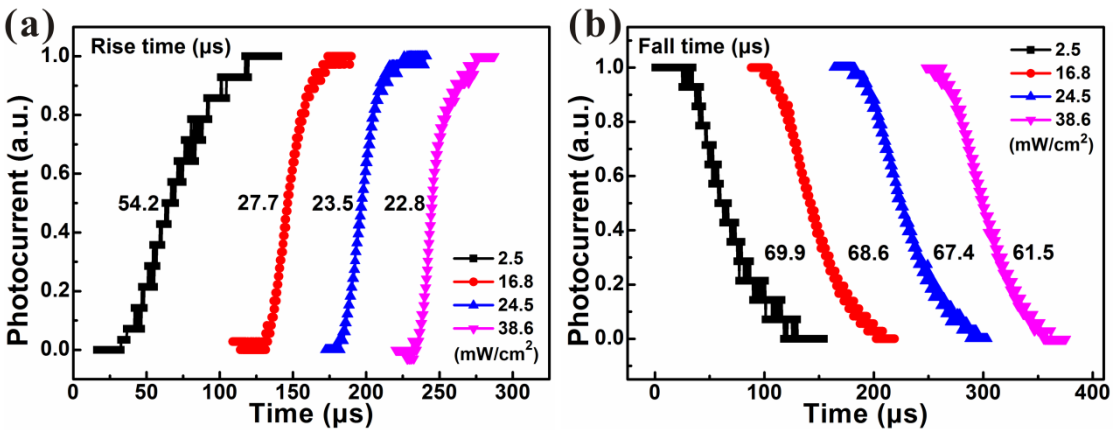

Fig. 6. (a) Rising and (b) falling edges of I-V curves at different light intensities (650 nm).

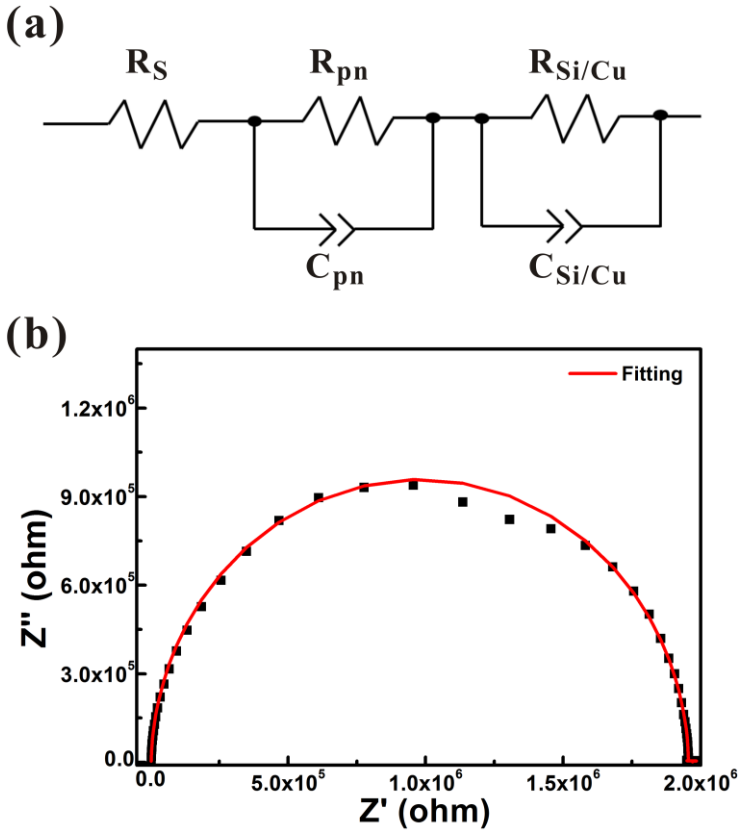

Fig.7. (a) The equivalent circuit model for the Nyquist plots. (b) Experimental impedance spectrum (Nyquist plots) of MoS_2/SiNWA heterojunction device.

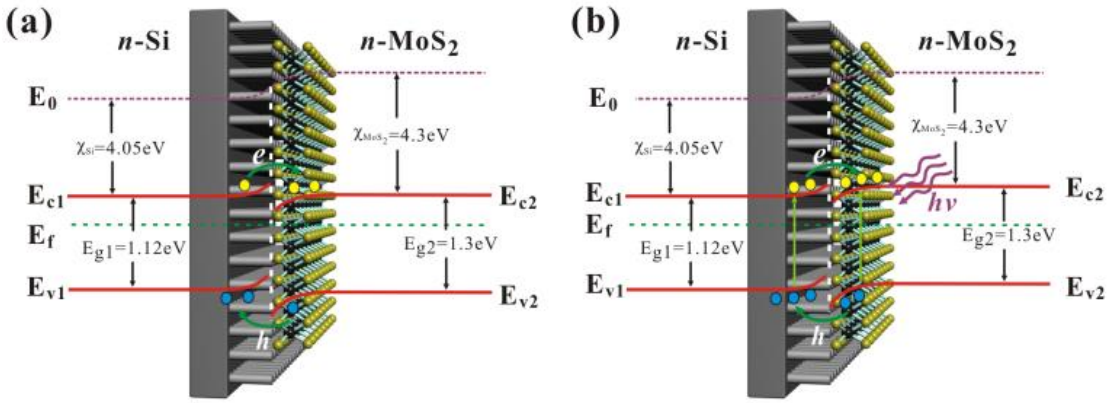

Fig. 8. Energy band diagrams of the MoS_2/SiNWA heterojunction (a) at equilibrium (in the dark condition), and (b) under light illumination.

Table 1. Summary of the device performances of five MoS_2/SiNWA PDs

Devices	I_{on}/I_{off}	Responsivity [A/W]	Detectivity [Jones]	Rise/fall time [μs]
1	1.1×10^5	53.5	2.8×10^{13}	2.9/7.3 (10 kHz) 22.8/61.5 (4 kHz)
2	0.98×10^5	49.2	1.95×10^{13}	31.3/67.5
3	1.22×10^5	48.6	2.25×10^{13}	25.6/72.1
4	1.54×10^5	51.8	2.54×10^{13}	23.6/67.6
5	1.63×10^5	55.6	3.19×10^{13}	26.5/76.7

Table 2. Summary of the device performances of the MoS_2/SiNWA PD and some reported PDs.

Devices type	I_{on}/I_{off}	Responsivity [A/W]	Detectivity [Jones]	Rise/Fall time [μs]	Ref.
MoS_2/SiNWA	1.1×10^5	53.5	2.8×10^{13}	2.9/7.3	This work
MoS_2/Si	59.9	11.9	2.1×10^{10}	30.5/71.6	[22]
MoS_2 Schottky PD	$\sim10^2$	0.57	$\sim10^{10}$	70/110	[41]
MoS_2/Gaphene	<1	0.032	/	$>10^6/10^6$	[47]
MoS_2/Black Phosphorus	/	22.3	3.1×10^{11}	15/70	[48]
WS2/Si	~10	5.7	/	670/998	[49]
Graphene/Si	$\sim10^4$	0.73	$\sim10^{12}$	320/750	[50]